

NAVAL POSTGRADUATE SCHOOL

Monterey, California



THESIS

**A WIDE ANGLE SPLIT-STEP
PARABOLIC EQUATION MODEL FOR
PROPAGATION PREDICTIONS OVER TERRAIN**

by

Konstantinos Vlachos

March, 1996

Thesis Advisor:

Ramakrishna Janaswamy

Approved for public release; distribution is unlimited.

DUDLEY KNOX LIBRARY
NAVAL POSTGRADUATE SCHOOL
MONTEREY CA 93943-5101

REPORT DOCUMENTATION PAGE			Form Approved OMB No. 0704	
Public reporting burden for this collection of information is estimated to average 1 hour per response, including the time for reviewing instruction, searching existing data sources, gathering and maintaining the data needed, and completing and reviewing the collection of information. Send comments regarding this burden estimate or any other aspect of this collection of information, including suggestions for reducing this burden, to Washington headquarters Services, Directorate for Information Operations and Reports, 1215 Jefferson Davis Highway, Suite 1204, Arlington, VA 22202-4302, and to the Office of Management and Budget, Paperwork Reduction Project (0704-0188) Washington DC 20503.				
1. AGENCY USE ONLY (Leave blank)		2. REPORT DATE March 1996		3. REPORT TYPE AND DATES COVERED Master's Thesis
4. TITLE AND SUBTITLE : A WIDE ANGLE SPLIT-STEP PARABOLIC EQUATION MODEL FOR PROPAGATION PREDICTIONS OVER TERRAIN			5. FUNDING NUMBERS	
6. AUTHOR(S) Konstantinos Vlachos				
7. PERFORMING ORGANIZATION NAME(S) AND ADDRESS(ES) Naval Postgraduate School Monterey CA 93943-5000			8. PERFORMING ORGANIZATION REPORT NUMBER	
9. SPONSORING/MONITORING AGENCY NAME(S) AND ADDRESS(ES)			10. SPONSORING/MONITORING AGENCY REPORT NUMBER	
11. SUPPLEMENTARY NOTES The views expressed in this thesis are those of the author and do not reflect the official policy or position of the Department of Defense or the U.S. Government.				
12a. DISTRIBUTION/AVAILABILITY STATEMENT Approved for public release; distribution unlimited			12b. DISTRIBUTION CODE	
13. ABSTRACT (maximum 200 words) The problem of radiowave propagation over irregular terrain is solved by using the wide angle parabolic equation method. The terrain is characterized by its height profile and its ground constants (here conductivity σ goes to infinity). We consider horizontal polarization and treat the ground as perfectly conducting (PEC) to simplify the formulation. This thesis uses a piece-wise conformal transformation to flatten the irregular terrain. The equations are solved by the split-step Fourier algorithm. A Hanning window is used both in spatial and in wavenumber domains to contain the computational domain. Effect of some numerical parameters such as the horizontal step size , height of the computational domain on the accuracy of the solution is investigated. The numerical results are compared with available results for some typical propagation problems.				
14. SUBJECT TERMS Propagation , Parabolic Equation , Conformal Mapping , Split- tep Fourier Algorithm.			15. NUMBER OF PAGES 53	
			16. PRICE CODE	
17. SECURITY CLASSIFICATION OF REPORT Unclassified	18. SECURITY CLASSIFICATION OF THIS PAGE Unclassified	19. SECURITY CLASSIFICATION OF ABSTRACT Unclassified	20. LIMITATION OF ABSTRACT UL	

Approved for public release; distribution is unlimited.

**A WIDE ANGLE SPLIT-STEP PARABOLIC EQUATION MODEL
FOR PROPAGATION PREDICTIONS OVER TERRAIN**

Konstantinos Vlachos
Lieutenant, Hellenic Navy
B.S.E.E., Hellenic Naval Academy, 1988

Submitted in partial fulfillment
of the requirements for the degree of

MASTER OF SCIENCE IN ELECTRICAL ENGINEERING

from the

**NAVAL POSTGRADUATE SCHOOL
March 1996**

170313
1/754
C.2

ABSTRACT

The problem of radiowave propagation over irregular terrain is solved by using the wide angle parabolic equation. The terrain is characterized by its height profile and its ground constants (here conductivity $\sigma \rightarrow \infty$). We consider horizontal polarization and treat the ground as perfectly conducting (PEC) to simplify the formulation. This thesis uses a piece-wise conformal transformation to flatten the irregular terrain. The equations are solved by the split-step Fourier algorithm. A Hanning window is used in both the spatial and wavenumber domains to contain the computational domain. Effect of some numerical parameters such as the horizontal step size, and height of the computational domain on the accuracy of the solution is investigated. The numerical results are compared with available results for some typical propagation problems.

TABLE OF CONTENTS

I.	INTRODUCTION.....	1
	A. BACKGROUND.....	1
	B. OBJECTIVE.....	2
II.	FORMULATION.....	3
	A. WIDE ANGLE PARABOLIC PARTIAL DIFFERENTIAL EQUATION...4	
	B. CONFORMAL MAPPING.....	6
	1. Conformal Mapping Approach.....	6
	2. Analytical Formulation of the Mapping.....	7
III.	SOLUTION PROCEDURE.....	9
	A. GENERATION OF THE TRANSFORMED SPACE.....	9
	B. NUMERICAL IMPLEMENTATION USING SPLIT-STEP FOURIER (SSF) ALGORITHM.....	10
IV.	RESULTS.....	13
	A. PROPAGATION OVER PEC PLANE.....	13
	B. PROPAGATION OVER PEC IN THE PRESENCE OF DUCT.....	14
	C. PROPAGATION OVER SPHERICAL EARTH.....	18
	D. PROPAGATION OVER PEC KNIFE-EDGE.....	21
	E. PARAMETRIC STUDY OF THE SSF ALGORITHM USING CONFOR- MAL MAPPING.....	22
V.	CONCLUSIONS.....	35

LIST OF REFERENCES.....	37
INITIAL DISTRIBUTION LIST.....	39

LIST OF TABLES

1. Mode numbers τ_n , for $\delta = \infty$ (PEC).....	19
---	----

LIST OF FIGURES

1. An Electric Source Producing Fields Over an Irregular Terrain	3
2. Transformation From W-Plane to ζ -Plane	4
3. Earth-Centered spherical Geometry	5
4. Terrain Flattening	7
5. Piece-Wise Conformal Mapping	8
6. Distribution of Points About a Slope Discontinuity	9
7. Marching in Range	10
8. Field Interpolation	12
9. Propagation Between Two Stations A and B, Both of Which are stationed over perfectly Conducting Ground.	13
10. Propagation Factor Versus the Horizontal Distance for a Source Placed at a Height of 5 m. Flat Earth, $f=1$ GHz and $\Delta x=5$ m.	15
11. Tri-linear surface elevated duct	16
12. Propagation Factor Versus the Receiver Height at a Range of 40 km in the Presence of a Tri-Linear Duct. Flat Earth, Transmitter Height = 30 m, $f=3$ GHz	17
13. Propagation Over Spherical Earth	18
14. Propagation Factor Versus Horizontal Distance Over Spherical Earth, $f = 300$ MHz, $\Delta x = 50$ m	20
15. Perfectly Conducting Knife Edge Between a Transmitter A and a Receiver B, Both of Which are on Perfectly Conducting Ground	21
16. Propagation Factor Versus the Receiver Height at a Range of 1 km. Smooth Earth, the Source Placed at a Distance of 500 m from the Edge, $\Delta z = 0.5$ m, $\Delta x = 0.75$ m and $z_{\max} = 255.5$ m	23
17. Propagation Factor Versus Receiver Height. $\Delta z = 0.5$ m, $\Delta x = 5$ m and $z_{\max} = 63.5$ m	24
18. Propagation Factor Versus Receiver Height. $\Delta z = 0.5$ m, $\Delta x = 2.5$ m and $z_{\max} = 63.5$ m	25

19.Propagation Factor Versus Receiver Height. $\Delta z=0.5$ m, $\Delta x =0.75$ m and $z_{\max}=63.5$ m	26
20.Propagation Factor Versus Receiver Height. $\Delta z=0.5$ m, $\Delta x =5$ m and $z_{\max}=127.5$ m	27
21.Propagation Factor Versus Receiver Height. $\Delta z=0.5$ m, $\Delta x =2.5$ m and $z_{\max}=127.5$ m	28
22.Propagation Factor Versus Receiver Height. $\Delta z=0.5$ m, $\Delta x =0.75$ m and $z_{\max}=127.5$ m	29
23.Propagation Factor Versus Receiver Height. $\Delta z=0.5$ m, $\Delta x =5$ m and $z_{\max}=255.5$ m	30
24.Propagation Factor Versus Receiver Height. $\Delta z=0.5$ m, $\Delta x =2.5$ m and $z_{\max}=255.5$ m	31
25.Propagation Factor Versus Receiver Height. $\Delta z=0.5$ m, $\Delta x =0.75$ m and $z_{\max}=255.5$ m	32

I. INTRODUCTION

A. BACKGROUND

Radiowave propagation over irregular terrain and in the presence of ducts is an extremely important topic in ground-to-ground as well as in ground-to-air communications. Similarly, the ability to predict radiowave propagation over irregular terrain has a significant impact in determining target detectability in a radar system. The physics of propagation is affected by ever-changing atmospheric conditions and by complex terrain features on the ground. The path between the transmitter and receiver is often obstructed by natural or man-made obstacles, such as hills, buildings, atmospheric layers, rain, etc. In these cases waves can reach the receiver along more than one path and the phenomenon is termed as multipath. In the case of atmospheric multipath fading, super-refraction or sub-refraction can lead to abnormal radiowave propagation, which can result in high gain or severe loss of signal. Reflection multipath fading, which is due to interference between the direct and the ground reflected waves, depends strongly on the terrain geometry. It is important to everyone involved with communications and radar systems to predict the electromagnetic fields due to radiating sources in the troposphere taking into account ducting and terrain effects.

Numerous analytical methods are available for predicting electromagnetic wave propagation, such as geometric optics, physical optics, normal mode analysis and combinations of the above. However, a complex environment complicates the application of some of these methods. The Parabolic Equation (PE) method has emerged as an extremely valuable method for assessing radiowave propagation in the lower atmosphere in the presence of ducts and over flat terrain, and for predicting radiowave propagation over sloping irregularities. One advantage of the parabolic Partial Differential Equation (PDE) is that the field at any location can be computed in terms of the field at a previous location. However, this would be accurate only when the waves propagate predominantly in the forward direction. This is approximately met in many propagation problems and is often assumed.

B. OBJECTIVE

In this thesis we adopt a wide angle parabolic equation due to Thomson-Chapman [Ref. 1] to predict radiowave propagation over an irregular terrain and in the presence of ducts. We consider horizontal polarization and treat the ground as perfectly conducting (PEC) to simplify the formulation. In practical situations this assumption will have minimal effect for frequencies in the VHF band and above. The key feature of this thesis is to use piece-wise conformal transformations to map the irregular terrain into a flat one and use known techniques available for flat terrain. It is in the transformed space rather than in the physical space that the parabolic approximation is made. Chapter II presents the derivation of the governing parabolic equation and the formulation of the conformal mapping. Chapter III details the generation of mesh in the transformed space and the numerical procedure for solving the PDE. The accuracy of the numerical solution is examined in Chapter IV. This includes a study on the effects of using different numerical values for various important parameters (e.g., step size, maximum height) on the accuracy of the solution and validation of the numerical results with known solutions for typical propagation problems. Recommendations and conclusions are presented in Chapter V.

II. FORMULATION

In this chapter we present theory on the governing parabolic equation and conformal mapping. Figure 1 shows a horizontally polarized dipole placed over an irregular, PEC terrain. The terrain is characterized by its height profile and its ground constants (here the conductivity $\sigma \rightarrow \infty$). We wish to solve the fields at a point over the ground in the presence of irregularities and ducts. We consider a 2-dimensional case where the source, geometry, refractivity profile, and all fields are y-invariant.

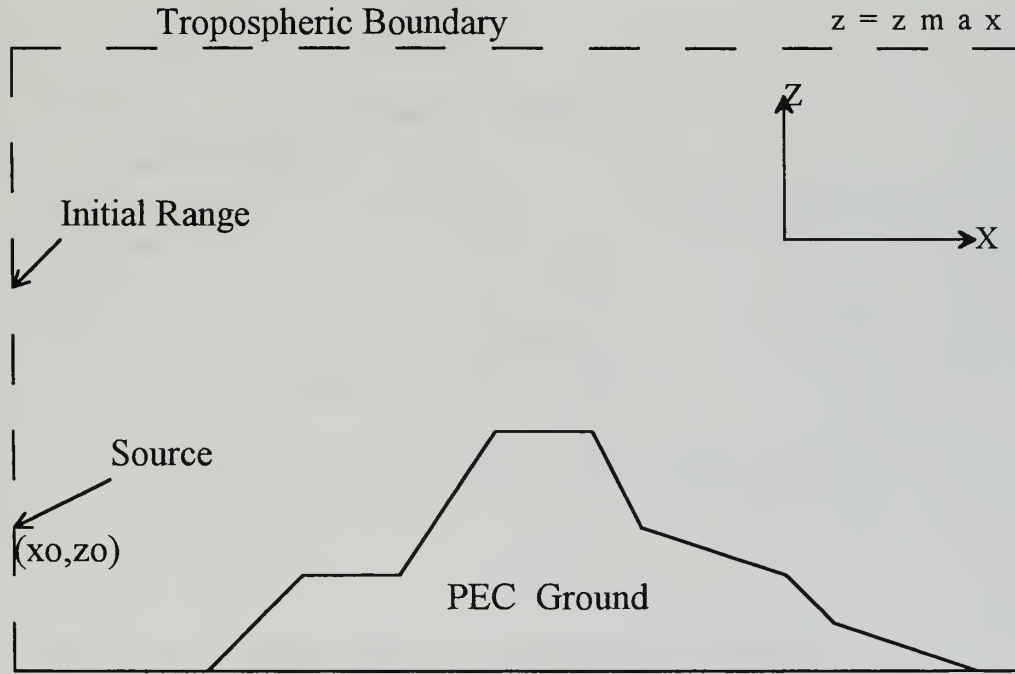


Figure 1. A source producing fields over an irregular terrain.

The terrain geometry is specified by means of discrete points, and straight line interpolation is assumed between the given data. The parabolic equation we present has to be finally solved numerically using either finite difference or Fourier transform approach. Both of these methods work best in a rectangular domain and a Cartesian mesh. Because the lower boundary is irregular, we cannot adopt a Cartesian mesh without discarding or adding points in going from one range step to the next. To avoid this situation, we will use

a coordinate transformation that will flatten the bottom boundary. Although there are multitudes of transformations available [Ref. 2], we have decided to use conformal mapping in our case. The advantage of using a conformal mapping is that it preserves the Laplacian operator without introducing undesirable cross-terms. This will be particularly advantageous when split-step Fourier transform approach is used to solve the PE. In this thesis, we use the split-step Fourier transform approach to solve the parabolic equation due to its superior computational performance. Our development parallels that of [Ref. 3].

A. WIDE ANGLE PARABOLIC PARTIAL DIFFERENTIAL EQUATION

Figure 2 shows the coordinate system used in the thesis.

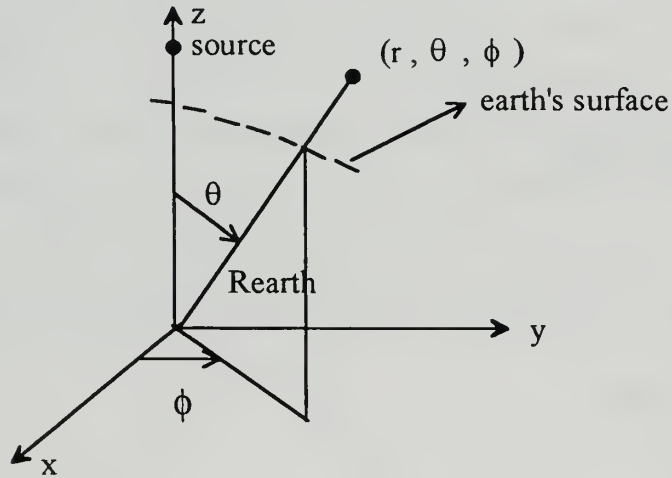


Figure 2. Earth-centered spherical geometry.

The starting point for our formulation is the earth flattened Helmholtz equation for the scaled field V [Ref. 4]:

$$\nabla_{xz}^2 V + k_o^2(1 + 2m)V = 0 \quad (1)$$

where $V(x,z) = \sqrt{x \sin \theta} E_\phi(x,z)$ for horizontal polarization, E_ϕ being the azimuthal component of the electric field, and (r,θ,ϕ) are the usual spherical coordinates. The center of the coordinate system is at the center of the earth and angle θ is measured from the

vertical line joining the center and transmitter location. The transmitter is assumed to be located at $\phi=0$ (Figure 2). Furthermore, $k_o = \omega \sqrt{\epsilon_o \mu_o}$, is the free space wavenumber, $x=r\sin\theta$ is the range variable, z is the height variable, and $m(x,z)=(n-1+z/a_e)$ is the modified refractive index of the atmosphere having an actual refractive index n , where a_e is the radius of the earth. In this chapter we include only the final details. Complete details can be found in [Ref. 5].

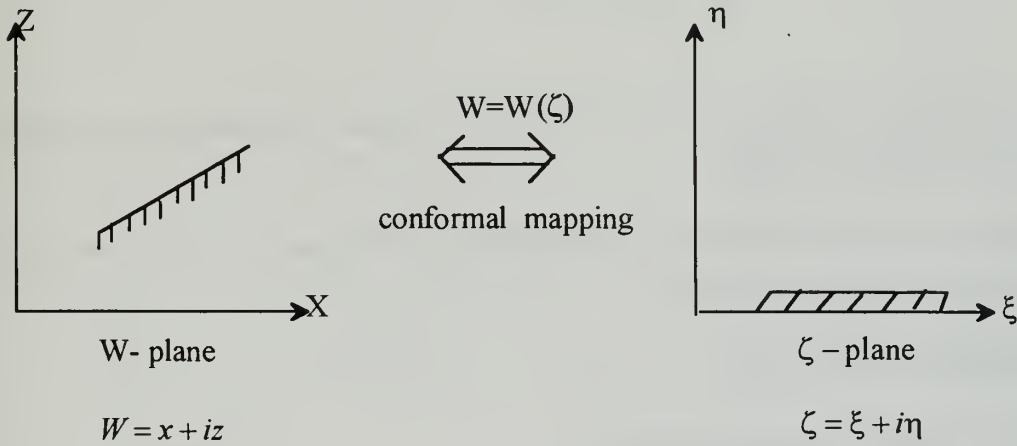


Figure 3. Transformation from W-plane to ζ -plane.

Under conformal mapping, [Fig. 3], equation (1) is transformed to:

$$\nabla_{\xi\eta}^2 V + k_o^2 |W'(\zeta)|^2 (1 + 2m) V = 0 \quad (2)$$

On expanding the Laplacian operator, equation (2) can be rewritten as

$$\frac{\partial^2 V}{\partial \xi^2} + \frac{\partial^2 V}{\partial \eta^2} + k_o^2 |W'(\zeta)|^2 (1 + 2m) V = 0, \quad (3)$$

where $|W'(\zeta)|$ is the Jacobian of the transformation and is given by

$$|W'(\zeta)| = \left| \left[\frac{1 - \sin(\frac{\pi\zeta}{\Delta r})}{1 + \sin(\frac{\pi\zeta}{\Delta r})} \right]^v \right| \quad (4)$$

Substituting $V = Ue^{ik_o\zeta}$, equation (3) can be simplified to:

$$\frac{\partial U}{\partial \xi} = ik_o(Q - 1)U \quad (5)$$

with $Q - 1 = \frac{1}{k_o^2} \frac{\partial^2}{\partial \eta^2} \frac{1}{(1 + \sqrt{1 + \frac{1}{k_o^2} \frac{\partial^2}{\partial \eta^2}})} + m$, and we have made the reasonable assumption

that $|W'(\zeta)| \approx 1$. For the transformation considered in this thesis, this is true everywhere except near points P and Q of Figure 5.

B. CONFORMAL MAPPING

1. Conformal Mapping Approach

A conformal mapping can transform an irregular polygonal shape into a rectangular one. We use a series of piece-wise conformal maps to transform the piecewise linear terrain to a flat one as shown in Figure 4.

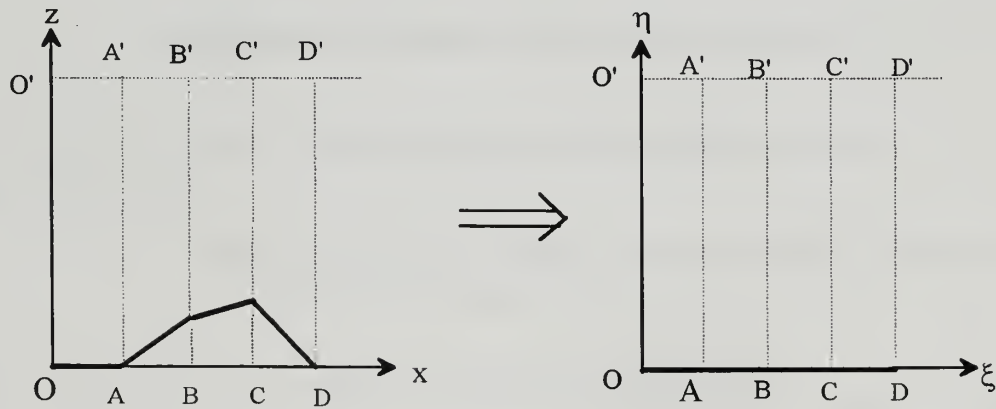


Figure 4. Terrain flattening.

For example, we conformally map the polygon A'ABBA' shown on the left to a corresponding rectangle shown on the right. Because the slope is different from one segment to the other, the mapping is also different. Detailed derivations of the mapping are given in [Ref. 5]. Here we present only the final results.

2. Analytical Formulation of the Mapping

Consider the transformation $W=f(\zeta)$ between the $W=r+iz$ and $\zeta=\xi+i\eta$ complex planes as shown in Figure 5.

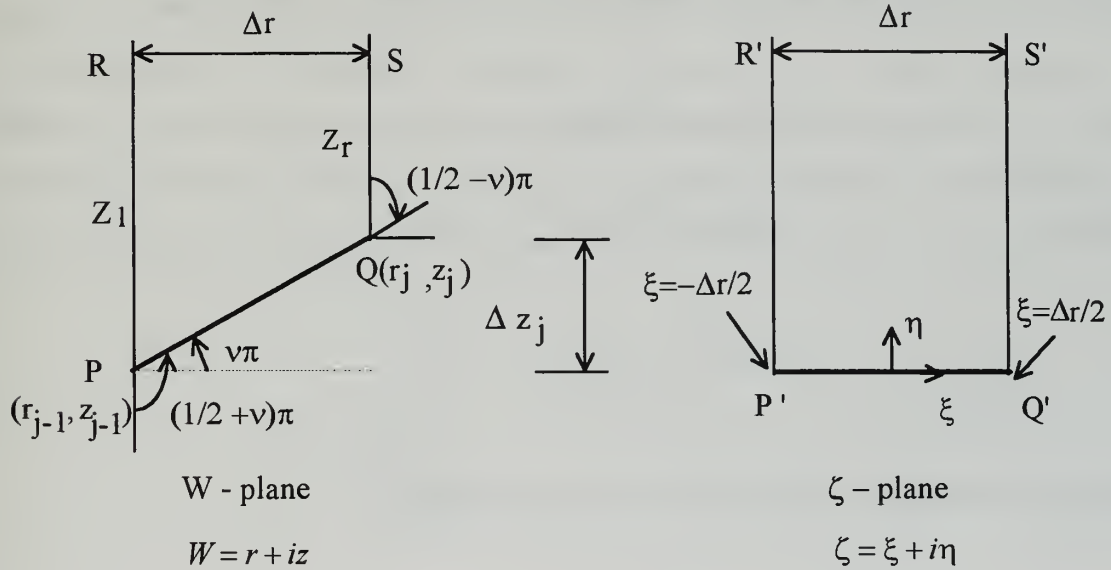


Figure 5. Piece-wise conformal mapping.

For the sake of simplicity we assume that the points R and S are at infinity. The mapping is given by the Schwarz-Christoffel formula [Ref. 3]:

$$W = W_P + \frac{\Delta r}{\pi} e^{iv\pi} \int_0^{\zeta_2} \frac{d\lambda}{\lambda^{v+\frac{1}{2}}(1-\lambda)^{\frac{1}{2}-v}} \quad (6)$$

where $\zeta_2 = \frac{1}{2}(\sin(\frac{\pi\zeta}{\Delta r}) + 1)$.

With reference to Figure 5, we define the slope parameter v as

$$v = \frac{1}{\pi} \left(\frac{\Delta z_j}{\Delta r} \right), \quad -\frac{1}{2} < v < \frac{1}{2}. \quad (7)$$

It is assumed that positive angles are measured in the counter clockwise direction. Points on the line PR' are mapped to the points on the line PR through:

$$z_l = z_{j-1} + \frac{\Delta r}{\pi} J(u; v) \quad (8)$$

where as points on the line $Q'S'$ are mapped to points on the line QS through:

$$z_r = z_j + \frac{\Delta r}{\pi} J(u; -v) \quad (9)$$

where

$$u = \tanh^2 \left(\frac{\pi \eta}{2 \Delta r} \right) = \frac{v}{1-v}, \quad \text{and}$$

$$J(u; v) = \int_0^u \frac{d\lambda}{\lambda^{\frac{1}{2}+v} (1-\lambda)^{\frac{1}{2}-v}}$$

Accurate formulas for computing $J(u; v)$ are given in [Ref. 5].

III. SOLUTION PROCEDURE

In the previous chapter we presented the underlying equations for the computation of fields over irregular/flat terrain and ducting conditions. In section A of the present chapter, we start with the generation of mesh points in the physical space. In section B, we continue with the numerical implementation using the split-step Fourier (SSF) algorithm for the final computation of the fields.

A. GENERATION OF THE TRANSFORMED SPACE

It is clear from equations (8) and (9) that a uniform mesh $\eta = k\Delta\eta$ in the transformed domain maps to different distribution of points on the vertical lines PR and QS. Furthermore, the distribution of points is dependent on the slope parameter ν . Therefore, in going from one range step to another, the distribution of points on the right side of the previous step will not coincide with the distribution of points on the left side of the present step. This is illustrated in Figure 6 for $\nu = 0.25$, $\Delta\eta = 2$ and $\Delta r = 25$ m, where

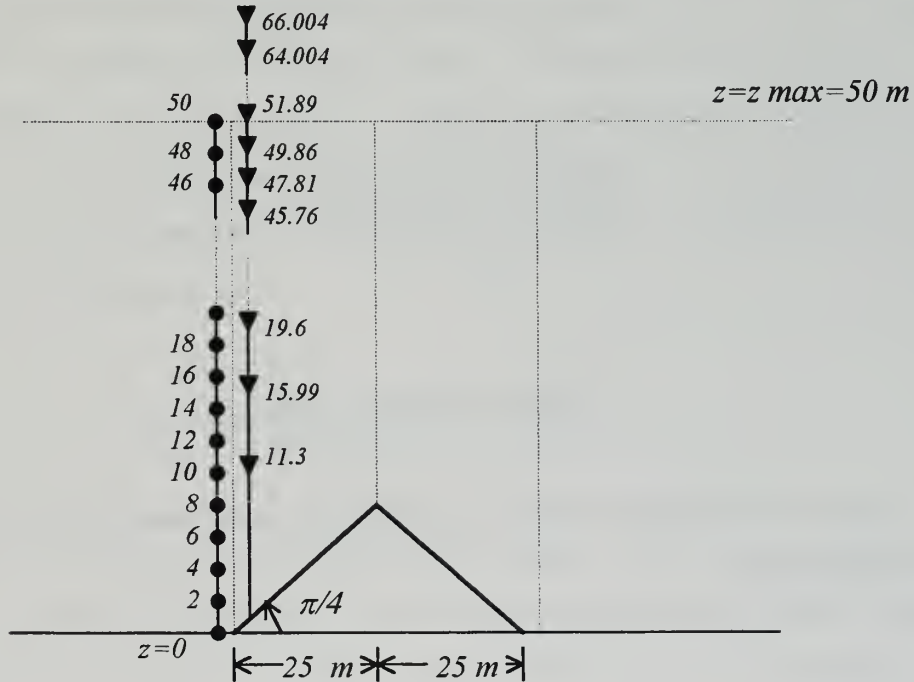


Figure 6. Distribution of points about a slope discontinuity.

points just to the left of triangle base are indicated by circles and points to the right of it by inverted triangles. Clearly interpolation or extrapolation of data is needed before the field values calculated at one range can be used as input for the next step. In this thesis, we use rational approximation, [Ref. 5] to do the desired interpolation.

B. NUMERICAL IMPLEMENTATION USING THE SPLIT-STEP FOURIER (SSF) ALGORITHM

Consider the parabolic partial differential equation given in equation (5). We would like to implement the equations by using the SSF algorithm. Figure 7 shows field U_- on a given vertical line. We would like to predict the field U_+ on a subsequent line spaced Δr from the original line.

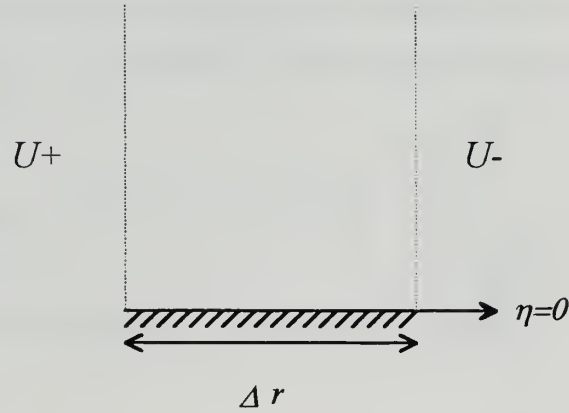


Figure 7. Marching in range.

To solve the parabolic equation, the following Fourier transform pair is used in the transformed domain:

$$\tilde{U}(\xi, p) = F(U) = \int_{-\infty}^{\infty} U(\xi, \eta) e^{ip\eta} d\eta \quad (10a)$$

$$U(\xi, \eta) = F^{-1}(\tilde{U}) = \frac{1}{2\pi} \int_{-\infty}^{\infty} \tilde{U}(\xi, p) e^{-ip\eta} dp \quad (10b)$$

The boundary condition $U(\xi, 0) = 0$ for horizontal polarization implies that $U(\xi, -\eta) = -U(\xi, \eta)$, $\eta > 0$, and $\tilde{U}(\xi, -p) = -\tilde{U}(\xi, p)$, $p > 0$. Using equation (10a) in equation (5) and making use of standard 'splitting of operators' [Ref. 2] we have:

$$\tilde{U}_+ = e^{-iA} \tilde{U}_- \quad (11)$$

where $A = \frac{\Delta r p^2}{k_o + \sqrt{k_o^2 - p^2}}$. The field in the spatial domain is obtained by inverse transformation and correcting for refractive effects:

$$U_+ = e^{ik_o m \Delta r} F^{-1}[e^{-iA} F[U_-]] \quad (12)$$

In computing the ordinary Fourier transform pair, we use a N-point FFT. Let us assume that the various quantities are band limited over $p_{\max} \leq p \leq p_{\max}$, and that the transform is evaluated at $p=0, \Delta p, 2\Delta p, \dots, (N-1)\Delta p$ where $\Delta p = 2\pi/(N\Delta z)$. Positive wavenumbers occur at $p=\Delta p, 2\Delta p, \dots, (N/2-1)\Delta p$ while negative wavenumbers occur at $(N/2+1)\Delta p, (N/2+2)\Delta p, \dots, (N-1)\Delta p$. The value $(N/2)\Delta p$ corresponds to both $+p_{\max}$ and $-p_{\max}$. We use a Hanning window to contain the computational domain at the top. The Hanning window is given by:

$$h(n) = \begin{cases} 1 & , 0 \leq n \leq \frac{3N}{8} \\ \sin^2\left(\frac{4\pi n}{N}\right) & , \frac{3N}{8} \leq n \leq \frac{N}{2} \end{cases} \quad (13)$$

We use it both in the spatial and wavenumber domains. A mirror image of $h(n)$ about $n=0$ is used for negative wavenumbers. Note that the Hanning window forces a gradual rolloff to zero over the last quarter of the domain. With the use of the Hanning window the solution of the parabolic equation can be written:

$$U_+ = e^{ik_o m \Delta r} F^{-1}[h(n)e^{-iA} F[h(n)U_-]] \quad (14)$$

As we mentioned at the begining of this chapter, because consecutive steps are taken in different transformed spaces, the calculated field at the right side of one range step cannot be directly used, in general, as input to the next step. For example, at the junction between flat and sloping terrain, points are uniformly distributed over a flat surface, but unevenly distributed over the sloping terrain. As mentioned previously, we use the rational approximation to calculate the field $f(z)$ at a desired point z , in terms of the fields f_- , f_+ and f_o at positions z_- , z_+ and z_o respectively as shown in Figure 8.



Figure 8. Field interpolation.

The field is interpolated as:

$$f(z) = (f_o + a_1(z - z_o))/(1 + b_1(z - z_o)). \quad (15)$$

where $a_1 = (f_+s_- - f_-s_+)/ (f_+ - f_-)$, $b_1 = (s_- - s_+)/ (f_+ - f_-)$ and $s_- = (f_o - f_-)/(z_o - z_-)$,

$$s_+ = (f_+ - f_o)/(z_+ - z_o).$$

IV. RESULTS

Having introduced the basic theoretical background, we now present the numerical results using the developed algorithm for several practical cases of radiowave propagation. We start with the prediction of propagation factor (excess loss over the free space case) over flat earth, with and without a duct. We compare our results with the exact solutions or with results available in the literature. The next case we consider is that of propagation over spherical earth in a non-refractive atmosphere. Finally, we present our solution for propagation over a knife-edge shaped obstacle. We use this terrain irregularity to comment on the overall accuracy of the method and its dependence on parameters, such as the step size for the marching and the maximum height chosen to truncate the computational domain.

A. PROPAGATION OVER A PEC PLANE

Consider a transmitter and a receiver at a height of 5 meters above flat ground and separated by 1 km, as shown in Figure 9.

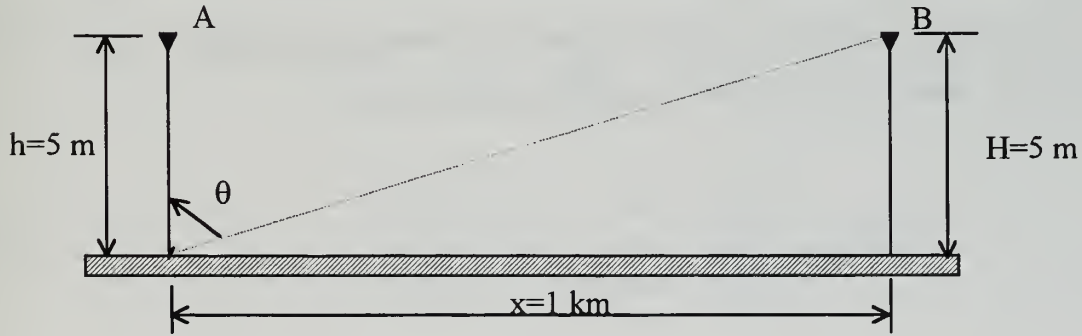


Figure 9. Propagation between two stations A and B, both of which are stationed over perfectly conducting ground.

In our numerical approach, the propagation factor, PF, is obtained from the normalized field, V, as [Ref. 6]

$$PF = 10 \log(|V|^2 x \lambda_o) \quad (16)$$

where x is the horizontal from the transmitter. A positive (negative) value of propagation factor implies gain (loss) with respect to propagation in free space. The exact solution can be obtained from image theory [Ref. 7, p. 144]. The expression valid in the far-field and for $x \gg h, H$ is $PF = |E/E_o| = 2 \sin(k_o h \cos \theta)$, where $\cos \theta = H/\sqrt{H^2 + x^2}$, h is the transmitter height, and H is the receiver height. The transmitter placed at $x=0, z=5$, where x, z are in meters. The frequency of operation is 1 GHz. We choose $N=1024$, $\Delta z = \Delta \eta = 0.15$ m and $\Delta x = \Delta r = 5$ m. The height of the upper boundary is $z_{\max} = 76.5$ m. The electric field is determined from the source line up to a distance of 1 km.

The variation of the propagation factor versus the horizontal distance is plotted in Figure 10. It is seen that there is a very good agreement with the image theory solution. For the first 50 m, the numerical solution differs slightly from the known solution. This is due to the breakdown of the condition $x \gg h, H$ in the image theory, far-field formula.

B. PROPAGATION OVER A PEC PLANE IN THE PRESENCE OF DUCT

Next we present the numerical results for radiowave propagation over a PEC plane, in the presence of a tri-linear duct [Figure 11] specified by

$$M(z) = \begin{cases} 340 + 0.118z & 0 \leq z \leq 135 \\ 499.03 - 1.06z & 135 \leq z \leq 150 \\ 322.33 + 0.118z & z \geq 150 \end{cases} \quad (17)$$

where z is in meters and $M = m \times 10^6$. This is a surface elevated duct with $\Delta M = 16$ and $\Delta h = 150$ m, where ΔM and Δh are defined at Figure 11. The minimum frequency (cut off frequency) required for propagation in the presence of this duct is 217 MHz. In our case the frequency of operation of 3 GHz is well above this cut off frequency. The height of the transmitter is 30 m and the maximum height is chosen to be $z_{\max} = 512$ m. We choose

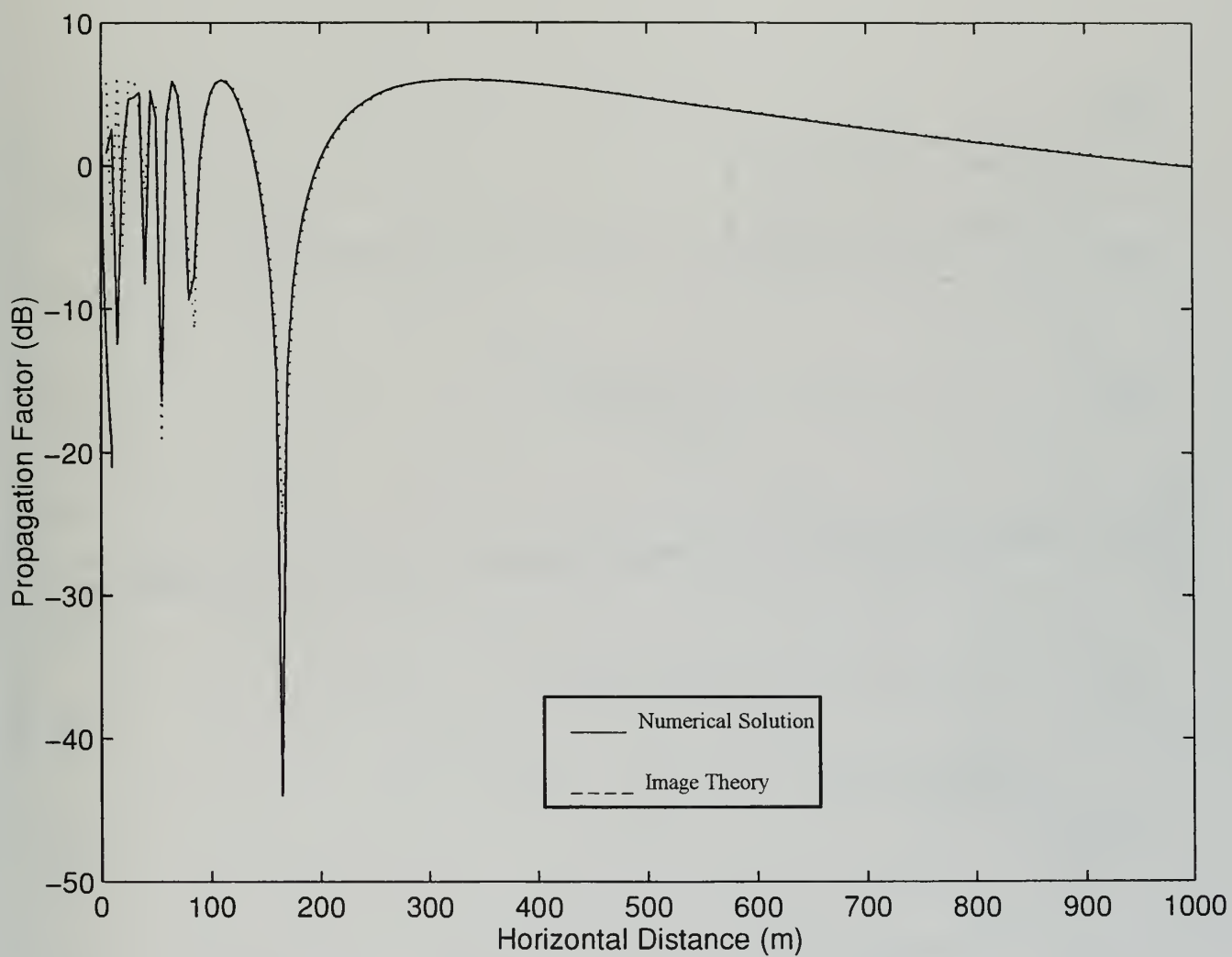


Figure 10. Propagation factor versus the horizontal distance for a source, placed at a height of 5 m. Flat earth, $f=1$ GHz, $\Delta x=5$ m and $H=h=5$ m.

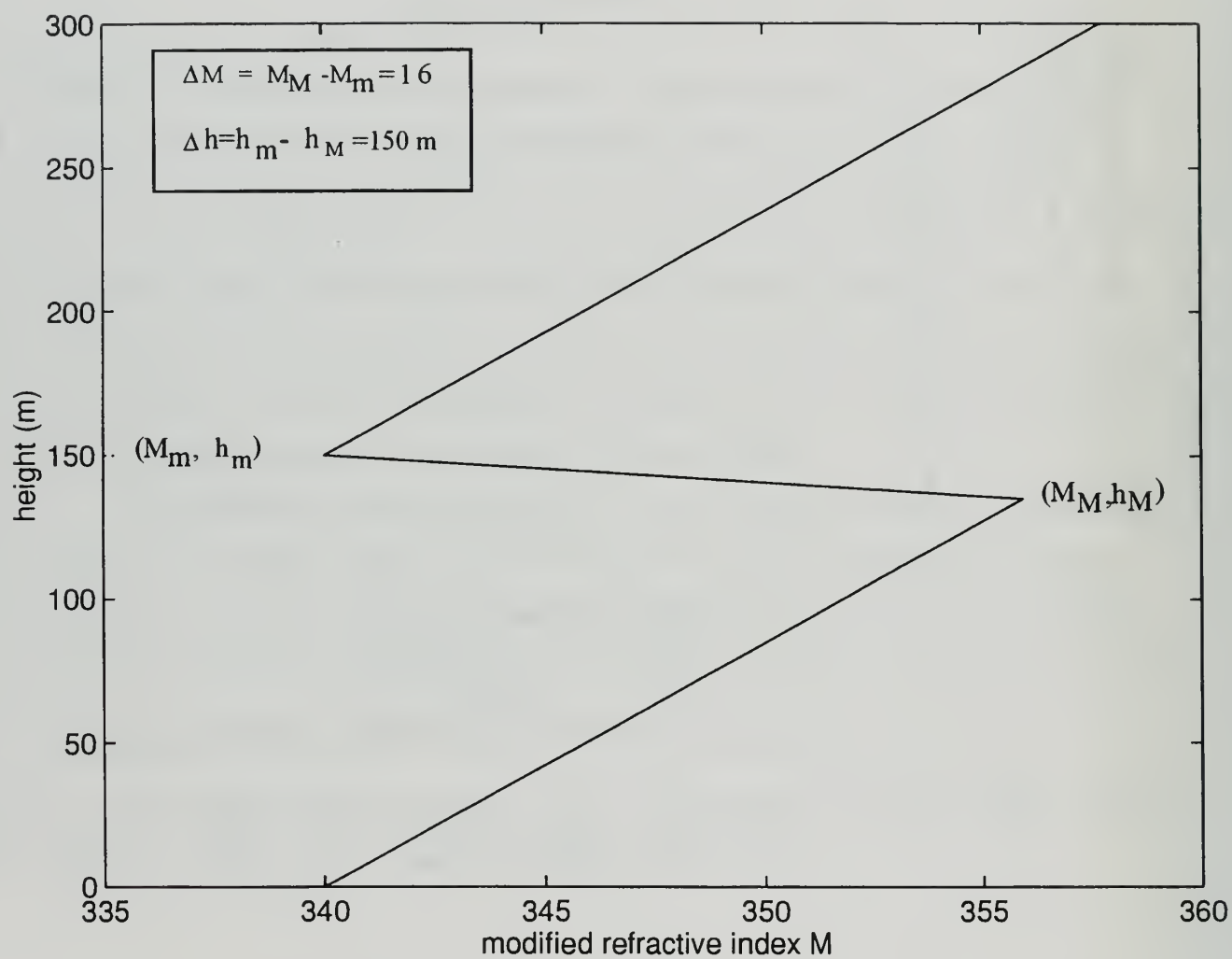


Figure 11. Tri-linear surface elevated duct.

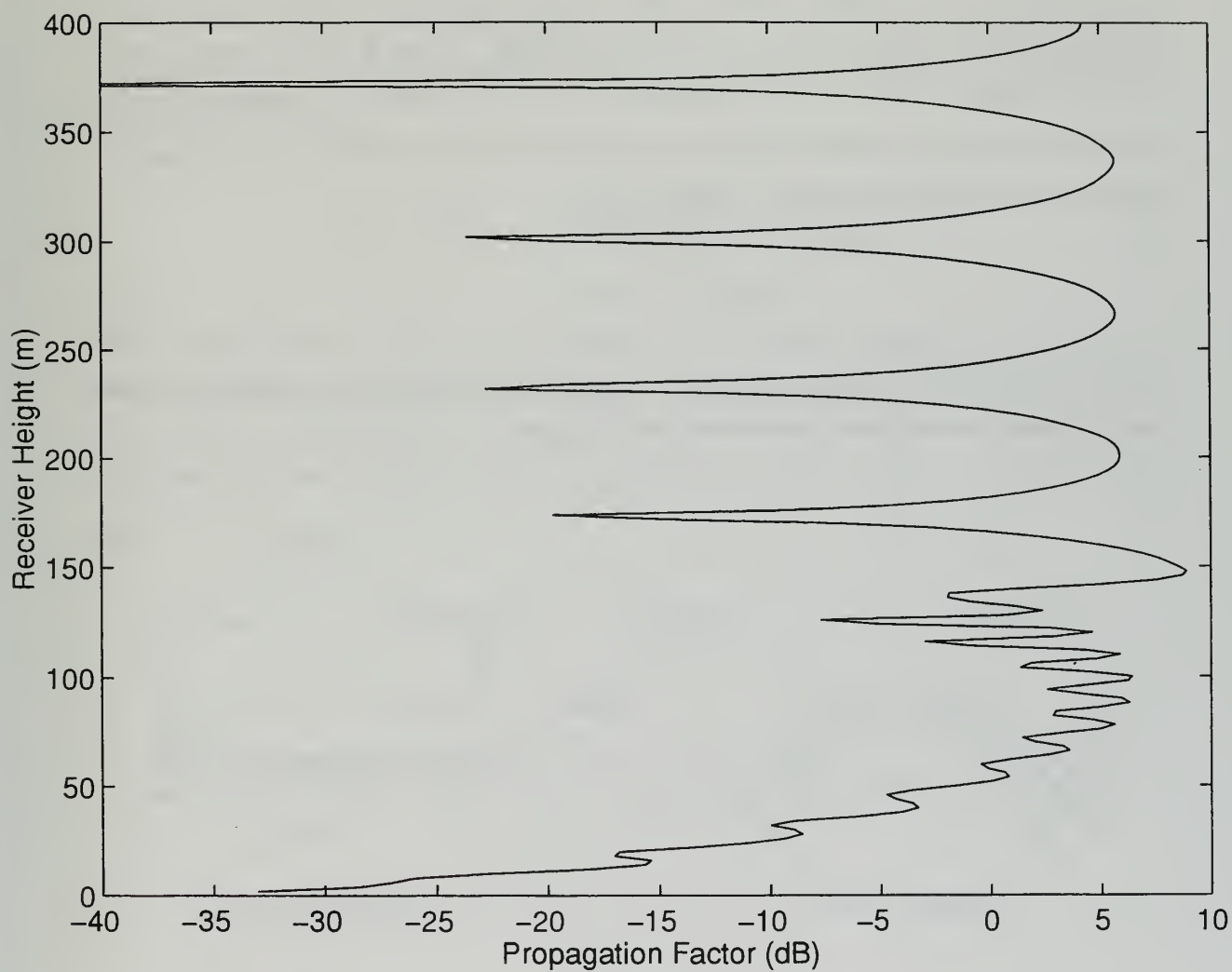


Figure 12. Propagation factor versus the receiver height at a range of 40 km in the presence of a tri-linear duct. Flat earth, transmitter height = 30 m, $f = 3$ GHz.

$N=512$, $Dz=2$ m and $Dx=200$ m. Figure 12 shows propagation factor versus the receiver height at a distance of 40 km. A favorable agreement with [Ref.6, Figure 3] is obtained.

C. PROPAGATION OVER SPHERICAL EARTH

Figure 13 shows a transmitter and a receiver located beyond the horizon over spherical earth. We consider transmitter and receiver antennas at heights of 10 m each. Distance to the horizon, d_T , from each station is $\sqrt{2hR_e}$, where R_e is the effective radius of the earth equal to 6375 km. In our case $d_T=11.3$ km. The situation described above is equivalent to the one where radiowaves propagate over flat earth but in the presence a modified atmosphere described by modified index

$$m(z) = (n - 1 + z/a_e) \quad (18)$$

where a_e is the radius of the earth, and we choose the refractive index, n , equal to 1. We use the equivalent model in our numerical calculations.

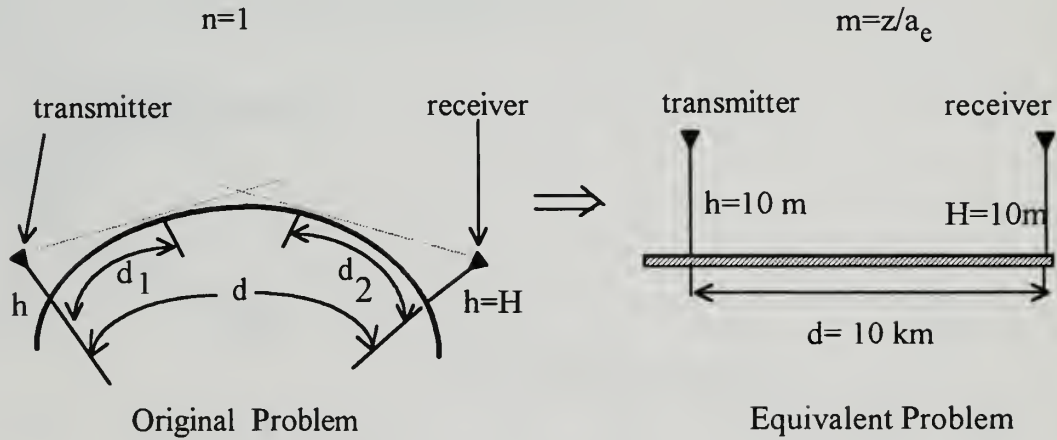


Figure 13. Propagation over spherical earth.

We consider a frequency of 300 MHz and treat the earth as a PEC. The exact solution to the problem can be obtained by using the mode theory [Ref. 8]. Our case pertains to the case of low antennas where the heights are less than the critical height h_c , defined by

$$h_c = 30\lambda_o^{\frac{2}{3}}, \lambda_o \text{ in m.} \quad (19)$$

In our case $h_c=30$ m at $f=300$ MHz. The distance d , must satisfy: $\lambda_o d > 2 h H$, meaning that the two stations must be at least 200 m apart. We use $N=1204$, $\Delta x=50$ m and $\Delta z=0.5$ m. This, places the maximum height at $z_{\max}=255.5$ m. We solve for the propagation factor as a function of the horizontal distance using our model and compare the result with the exact solution [Ref. 8]

$$PF = |E/E_o| = 2\sqrt{2\pi\zeta} \left| \sum_{n=1}^{\infty} \frac{e^{-i\tau_n\zeta}}{\delta+2\tau_n} f_n(h)f_n(H) \right| \quad (20)$$

where $\delta = [k_o R_e]^{\frac{2}{3}}(\epsilon_{rc} - 1)$, $\epsilon_{rc} = \epsilon_r - i\sigma_r$ where ϵ_r is the relative permittivity and σ_r is the relative conductivity, $\zeta = sd$, $s = [k_o/R_e^2]^{\frac{1}{3}}$, τ_n = complex numbers which depend on δ , and $f_n(h)$, $f_n(H)$ are height gain functions for the n -th mode (term). For low antennas $f_n(x)$ is independent of n and is given by $f(x) = 1 + ik_o x \sqrt{\epsilon_{rc} - 1}$. The constants τ_n are given as in

Table 1:

n	τ_n
1	$1.856e^{-i\pi/3}$
2	$3.245e^{-i\pi/3}$
3	$4.382e^{-i\pi/3}$
>3	$0.5[3\pi(n+0.25)]^{2/3}e^{-i\pi/3}$

Table 1. Mode numbers τ_n for $\delta=\infty$, (PEC).

In Figure 14 we plot the propagation factor versus the horizontal distance d for a range up to 10 km. There is a very good agreement with the modal solution, beyond the first 400 m. It was already mentioned that the distance between the two stations has to be

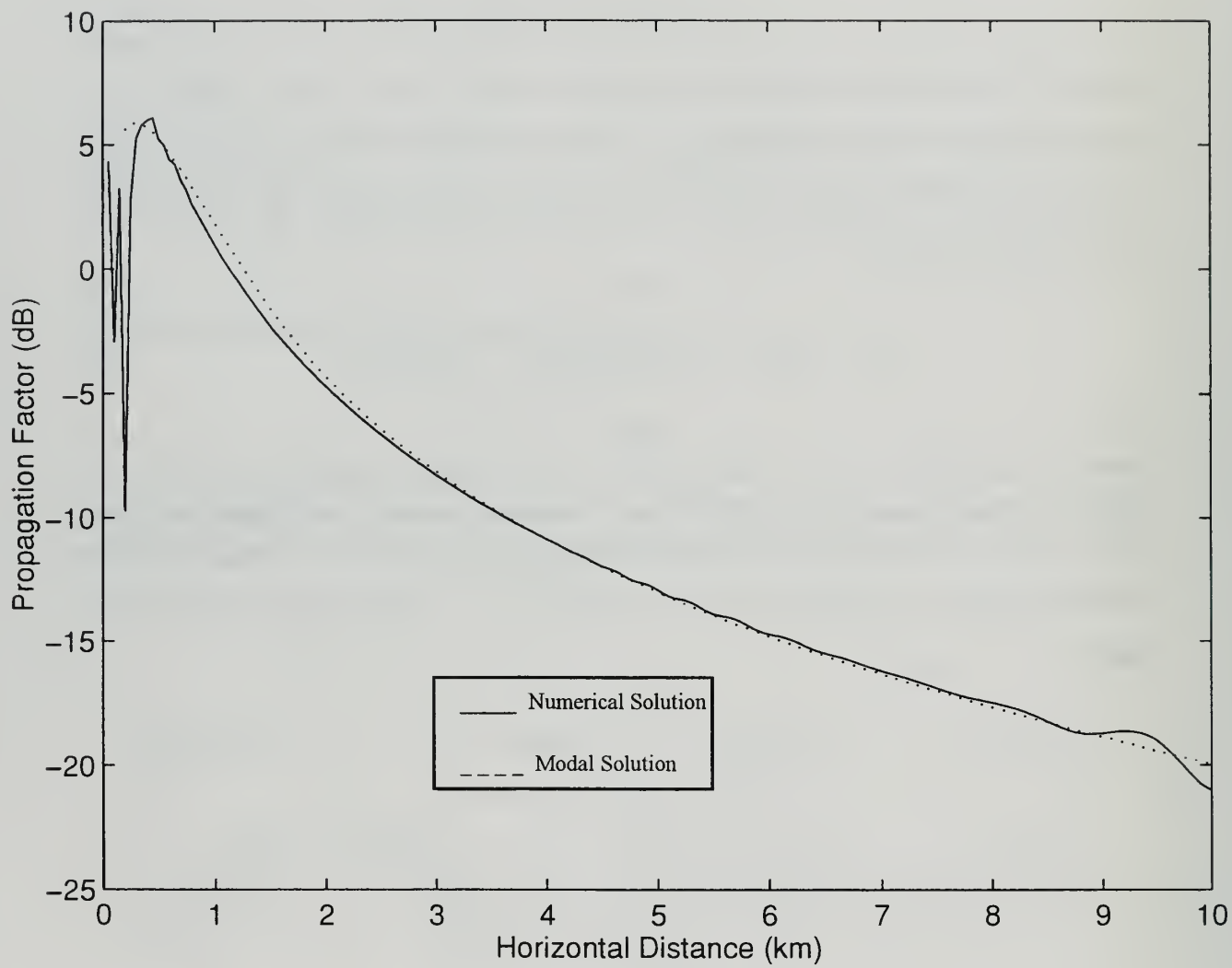


Figure 14. Propagation factor versus horizontal distance over spherical earth, $f=300$ MHz, $\Delta x=50$ m.

greater than 200 m in the modal solution, which explains the disagreement for the first few hundred meters.

D. PROPAGATION OVER PEC KNIFE-EDGE

The final example we consider is that of propagation over a knife edge on a conducting plane. Consider a perfectly conducting knife-edge of height 25 m, as shown in Figure 15.

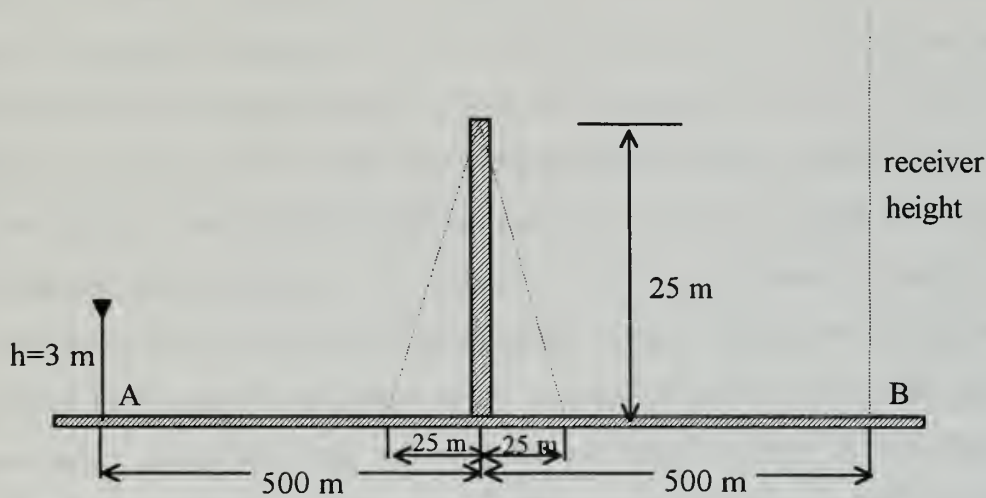


Figure 15. Perfectly conducting knife edge between the transmitter at A and the receiver B, both of which are on perfectly conducting ground.

We compare our numerical solution with a four ray model of knife edge diffraction theory [Ref. 9]. The two stations are at distances d_1 and d_2 from the plane of the edge. We choose $d_1 = d_2 = 500$ m. In the parabolic equation computations, we replace the knife edge with a triangular hill having a base of 50 m (Figure 15). The source is placed at a height of 3 m and we would like to determine the propagation factor as a function of receiver height. We choose a maximum height of 255.5 m, and the other parameters as: $N=1024$,

$\Delta z=0.5$ and $\Delta x=1$ m. The frequency of operation is 300 MHz. The numerical results are plotted in Figure 16, along with the four-ray solution, [Ref. 9]. There is an excellent agreement between the two plots.

E. PARAMETRIC STUDY OF THE SSF ALGORITHM USING CONFORMAL MAPPING

We use the knife edge irregularity to show the dependence of the solution on the following parameters: the horizontal step size and the maximum height chosen. We choose three different heights, each of which corresponds to the following values of N (with fixed vertical step size $\Delta z=0.5$ m): $N=256$, 512 and 1024 . The values of height are: $z_{\max}=63.5$, 127.5 and 255.5 meters respectively. For each of these heights, we create three sets of plots, for three different values of the horizontal step sizes: $\Delta x=5$, 2.5 and 0.75 meters. In Figures 17, 20 and 23 ($\Delta x=5$ m), we discuss the effect of the maximum height chosen for fixed Δx and it is seen that $z_{\max}=76.5$ m (Figure 17) is certainly not high enough. Only if we use higher a computational domain (Figures 20 and 23) do we obtain a solution which has resemblance with the four-ray solution. In the second set of Figures for a fixed $\Delta x=2.5$ m, (Figures 18, 21 and 24), again we conclude that the higher the z_{\max} the better the agreement between the numerical and the four ray solution. In Figures 21 and 24 (z_{\max} equal to 125.5 and 255.5 , respectively) we start to obtain a solution similar to the four-ray theory solution, but not yet an accurate one. Finally in Figures 19, 22 and 25, for the fixed horizontal step size $\Delta x=0.75$ m, we see that the solution with z_{\max} of 125.5 m or 255.5 m (Figures 22 and 25) produces very good agreement.

Next we discuss the effect of the horizontal step size Δx for a fixed vertical step size Δz and z_{\max} (N). In Figures 17 through 19 the maximum height is 76.5 m and $\Delta z=0.5$ m. We see that even for very small Δx , an acceptable solution is not obtained. In this case the solution is dominated by the height parameter (not convergent yet). In Figures 20 through 22, we use $z_{\max}=125.5$ m and $\Delta z=0.5$ m. It is seen that as we decrease the horizontal step size a better agreement with the four-ray solution is achieved (Figure 22). Figures 23 through 25 present the results for a fixed $\Delta z=0.5$ m and $z_{\max}=255.5$ m. Again

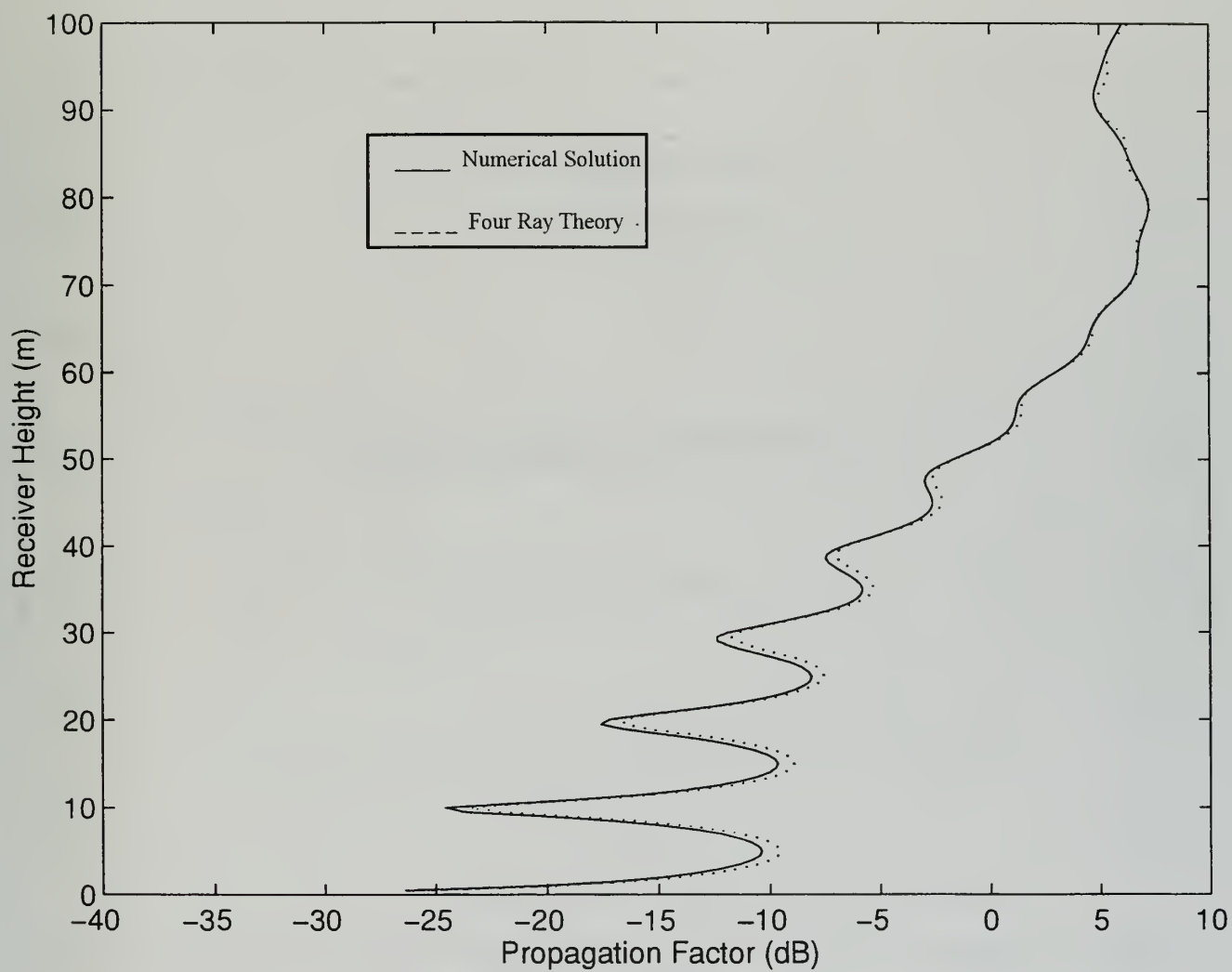


Figure 16. Propagation factor versus the receiver height at a range of 1 km. Smooth earth, the source placed at a distance of 500 m from the edge. $\Delta z=0.5$ m, $\Delta x=0.75$ m and $z_{\max}=255.5$ m.

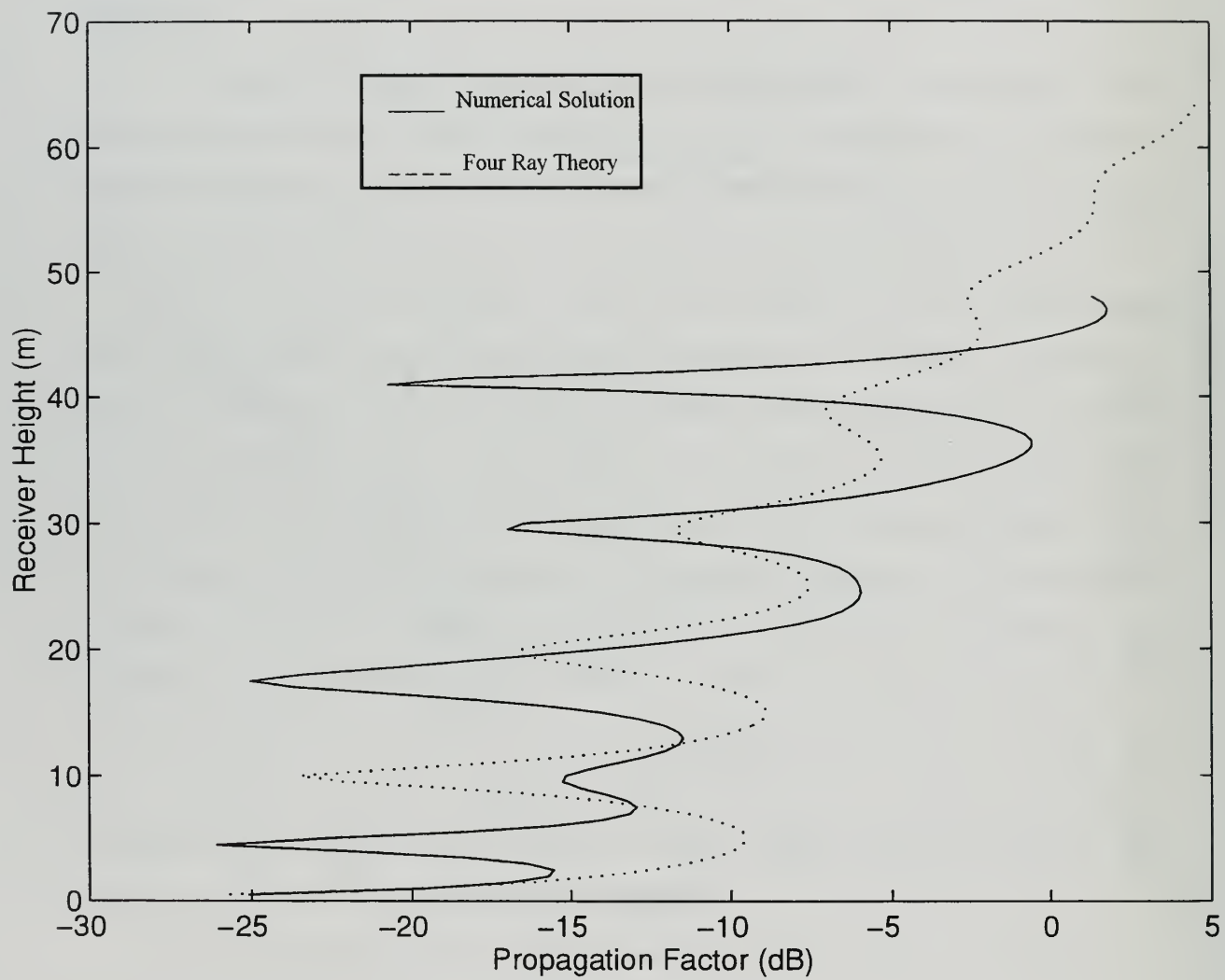


Figure 17. Propagation factor, PF, versus the receiver height. $\Delta z = 0.5$ m, $\Delta x = 5$ m and $z_{\max} = 63.5$ m.

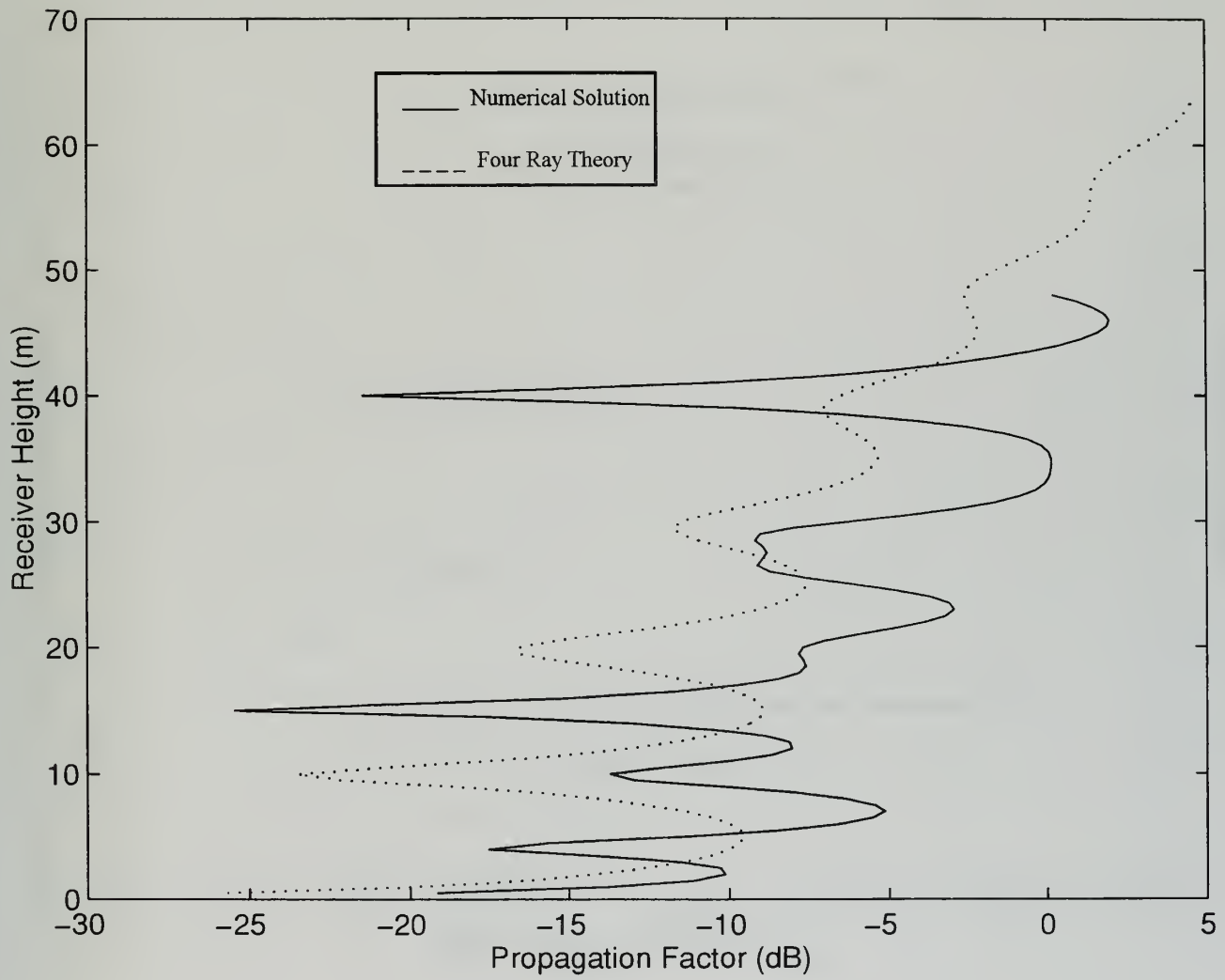


Figure 18. Propagation factor versus the receiver height. $\Delta z = 0.5$ m, $\Delta x = 2.5$ m and $z_{\max} = 63.5$ m.

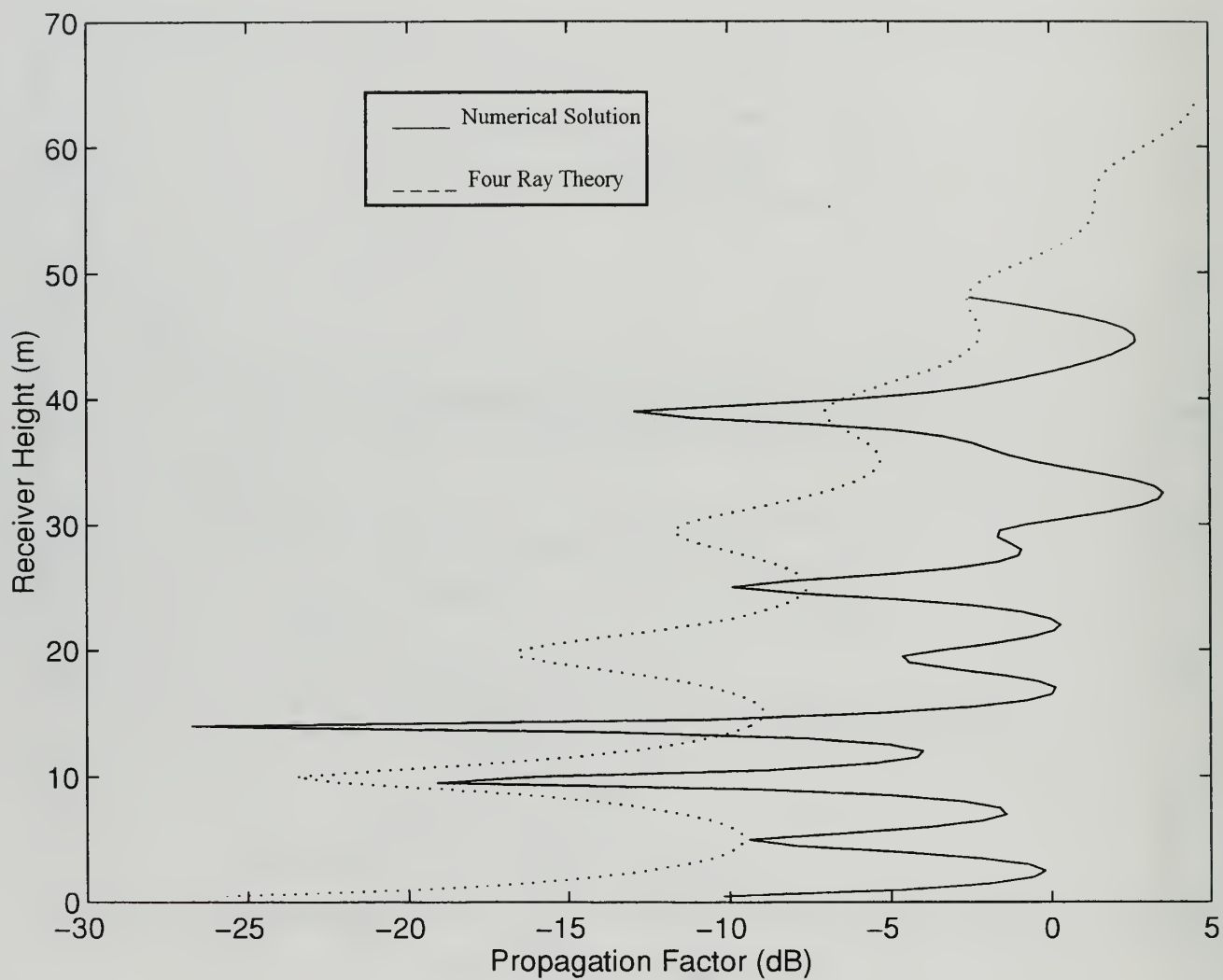


Figure 19. Propagation factor versus the receiver height. $\Delta z = 0.5$ m, $\Delta x = 0.75$ m and $z_{\max} = 63.5$ m.

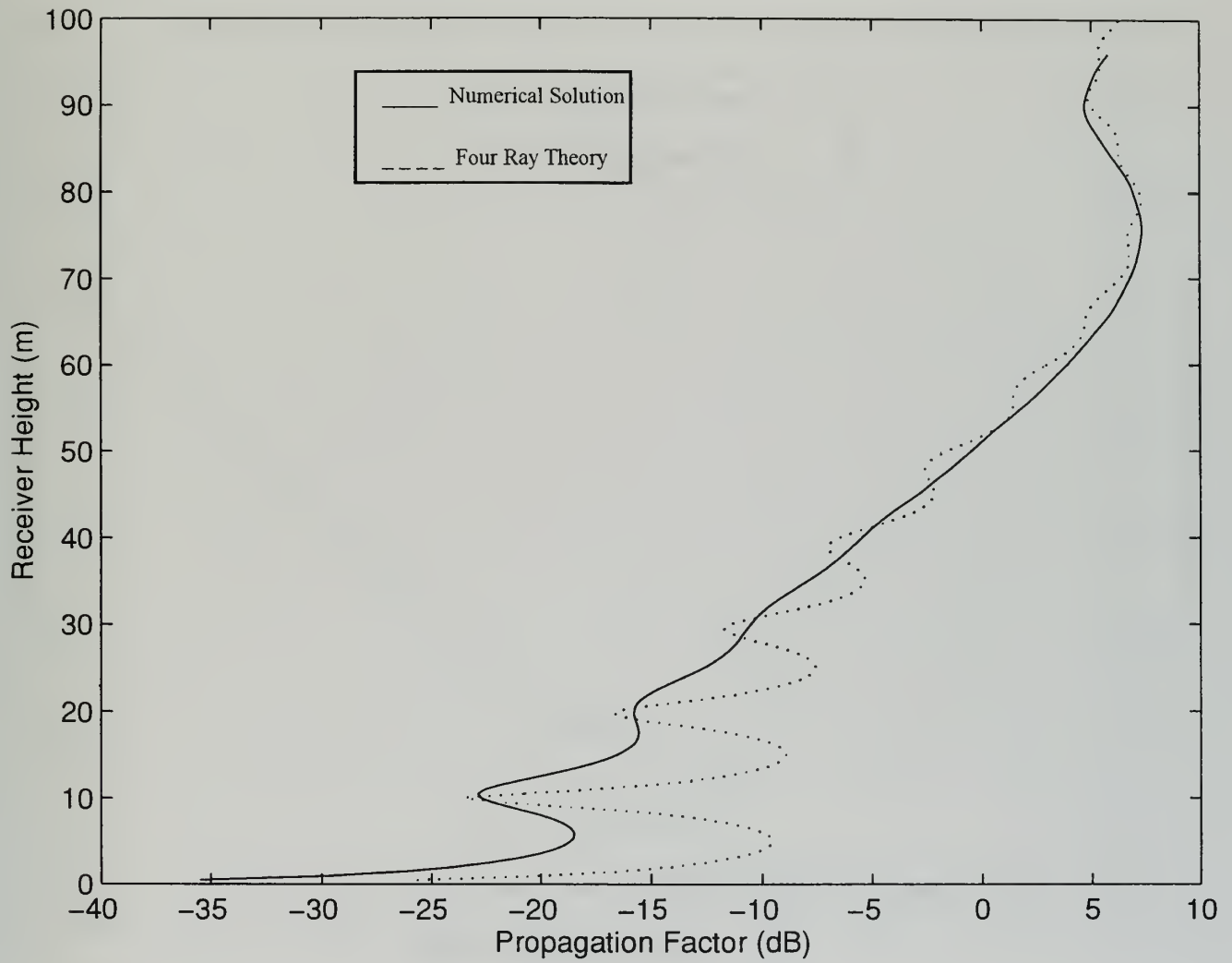


Figure 20. Propagation factor versus the receiver height. $\Delta z = 0.5$ m, $\Delta x = 5$ m and $z_{\max} = 127.5$ m.

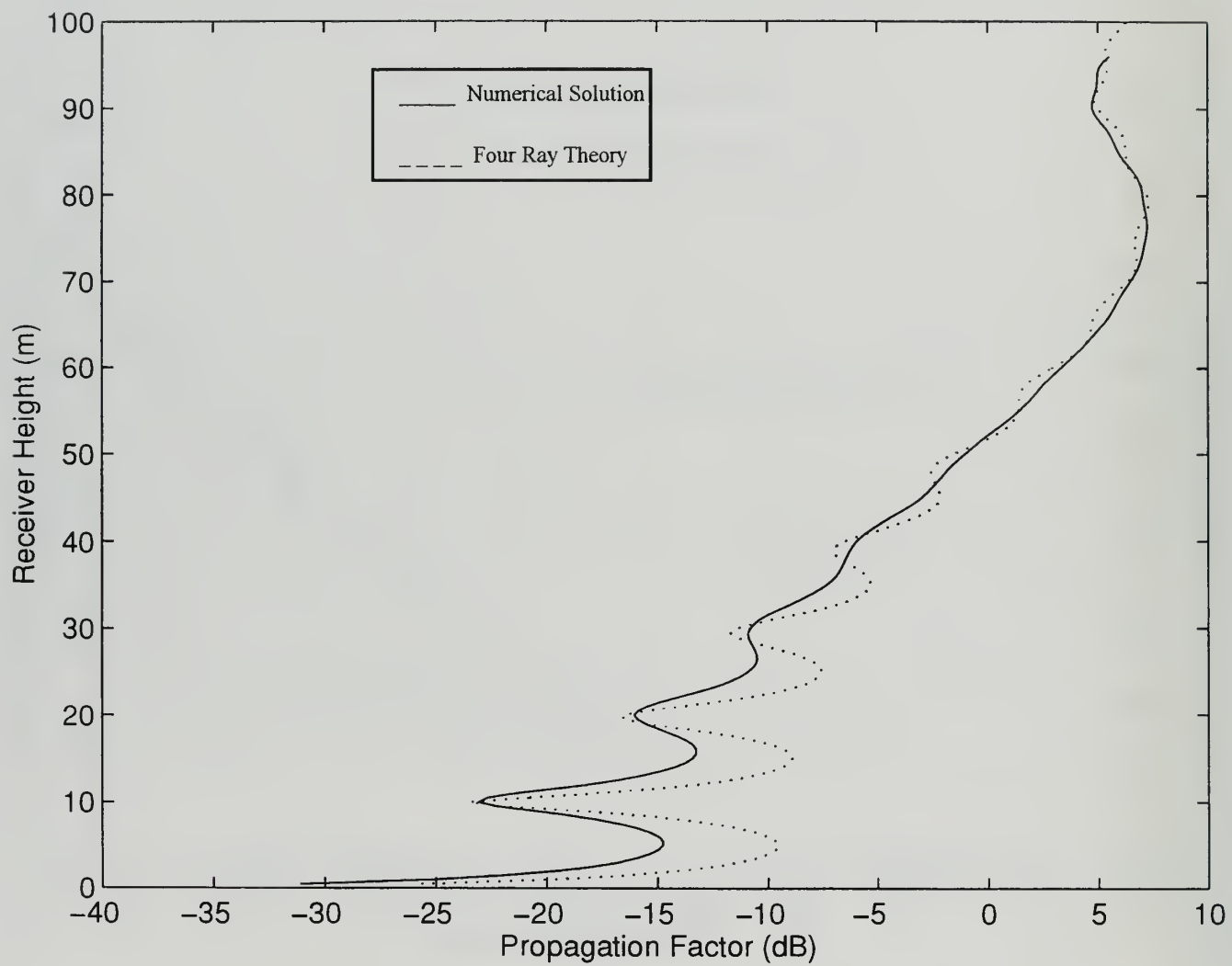


Figure 21. Propagation factor versus the receiver height. $\Delta z = 0.5$ m, $\Delta x = 2.5$ m and $z_{\max} = 127.5$ m.

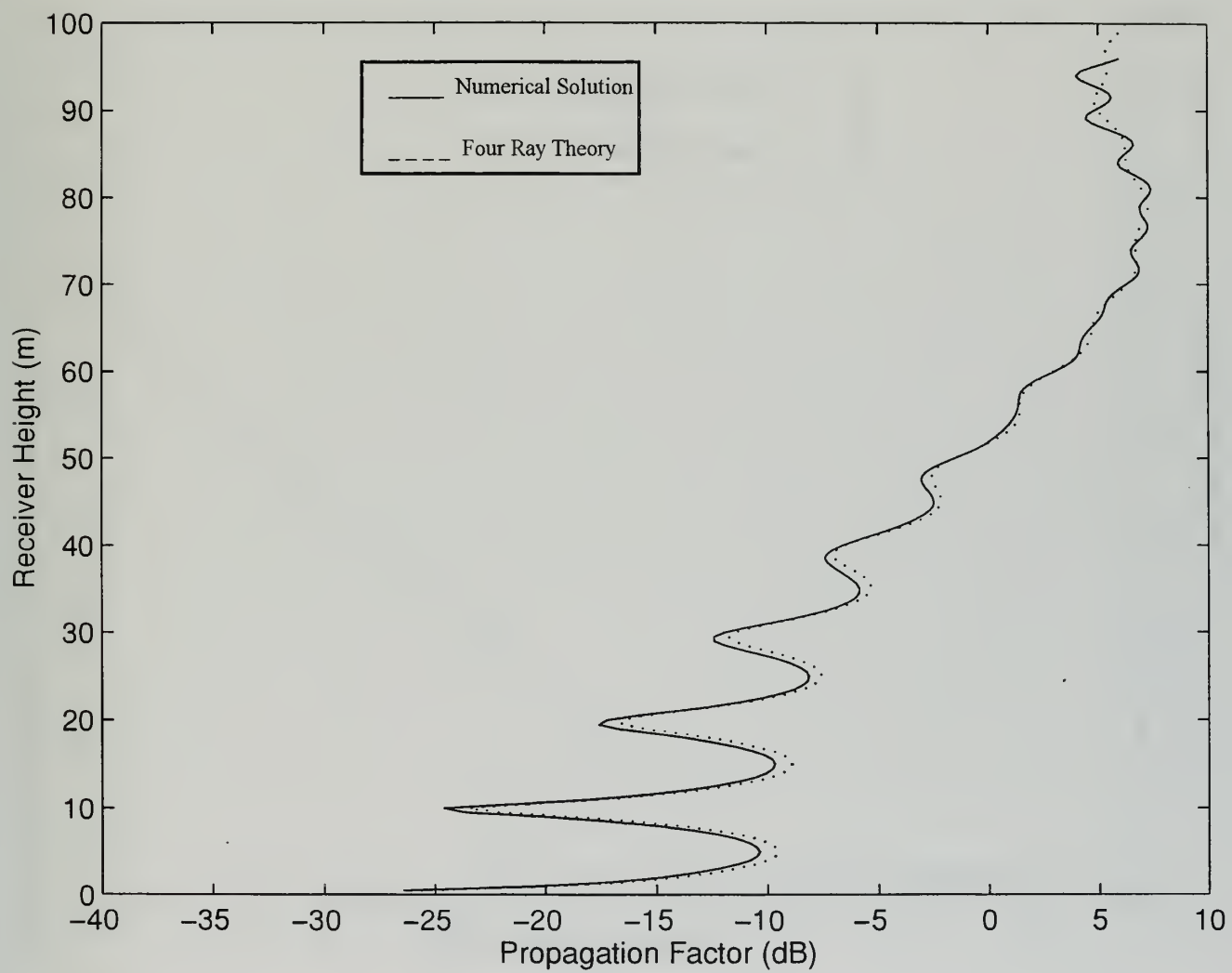


Figure 22. Propagation factor versus the receiver height. $\Delta z=0.5$ m, $\Delta x=0.75$ m and $z_{\max}=127.5$ m.

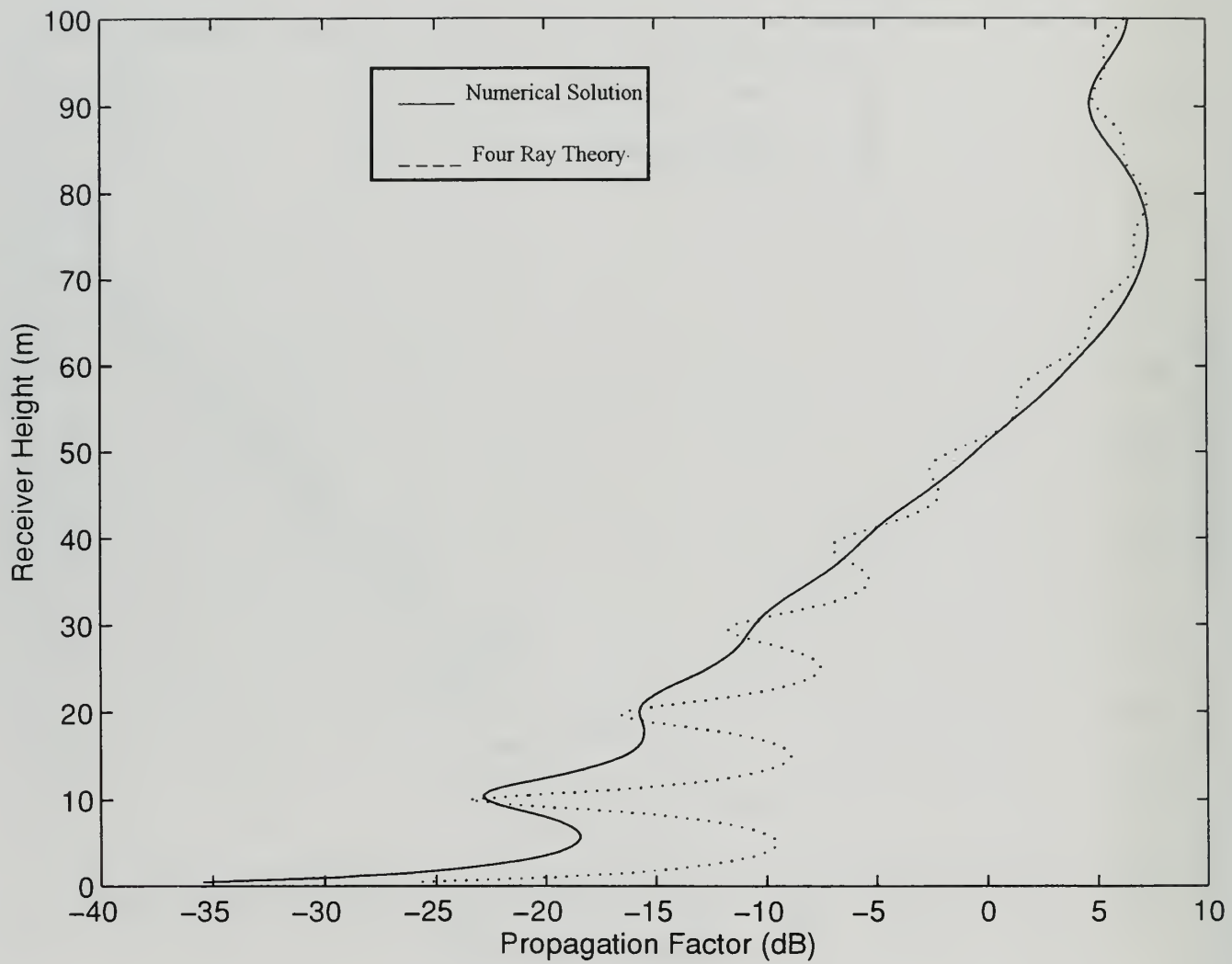


Figure 23. Propagation factor versus the receiver height. $\Delta z = 0.5$ m, $\Delta x = 5$ m and $z_{\max} = 255.5$ m.

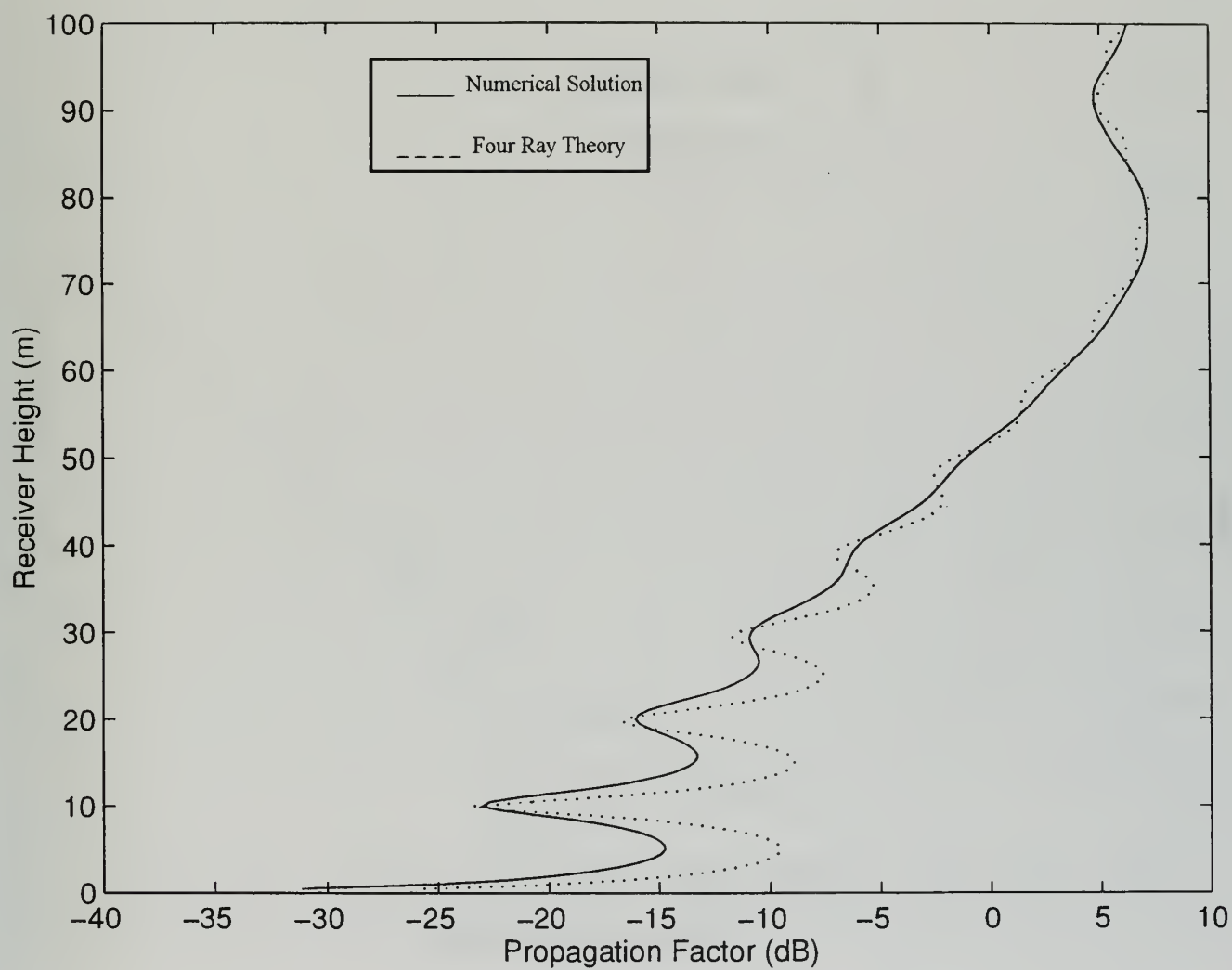


Figure 24. Propagation factor versus the receiver height. $\Delta z = 0.5$ m, $\Delta x = 2.5$ m and $z_{\max} = 255.5$ m.

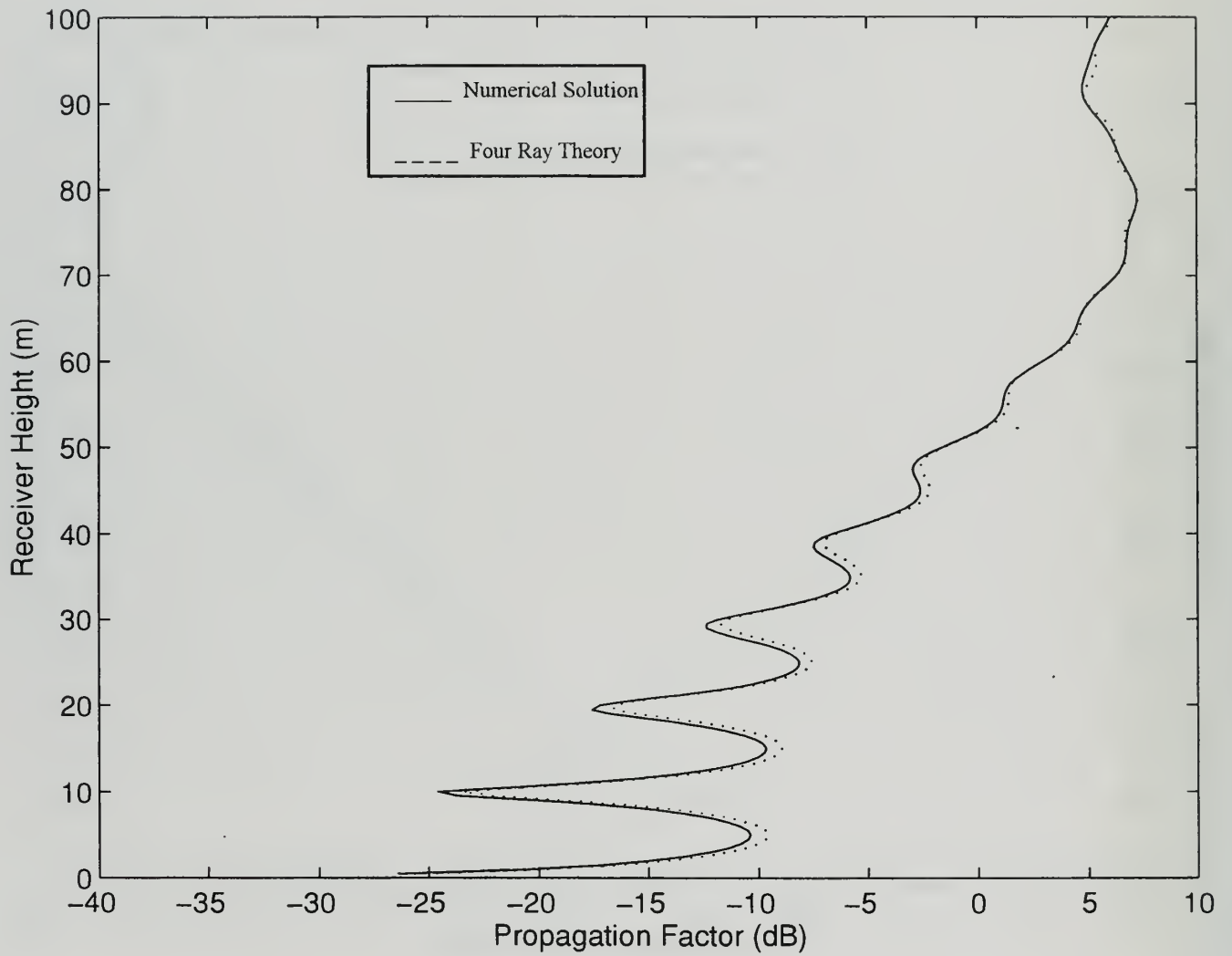


Figure 25. Propagation factor versus the receiver height. $\Delta z=0.5$ m, $\Delta x=0.75$ m and $z_{\max}=255.5$ m.

the effect of Δx is easily seen and Figure 25 shows a numerical solution with an excellent agreement with the four-ray theory solution.

V. CONCLUSIONS

In this thesis, a numerically efficient method to model radiowave propagation over irregular terrain and in a stratified atmosphere, using the parabolic equation, was implemented and tested. The parabolic equation method is a full-wave method, and aspects such as forward reflection, refraction, diffraction, and surface wave propagation are included. However, it ignores back-scattering. Since it ignores back propagation, it allows for a rapid solution of the fields using marching techniques along the propagation path starting from the source. It offers an advantage compared to the ray method in that it is valid in the shadow region where the latter method completely breaks down. Furthermore, it is the most practical method for predicting propagation over long ranges (thousands of wavelengths).

After presenting the wide angle parabolic equation, we presented a piece-wise conformal transformation to map the irregular terrain into a flat one, so that known techniques available for flat terrain can be used. The split-step Fourier (SSF) algorithm was used in the computational domain to solve the parabolic PDE. A Hanning window was used both in the spatial and wavenumber domains. Although very small step sizes were used for marching along ranges of several kilometers, the method is very time efficient. Horizontal polarization was considered and the ground was treated as a perfect electric conductor (PEC) to simplify the formulations. This assumption will have minimal effect in practical situations and for frequencies in the VHF band and above.

Numerical results to predict radiowave propagation for several practical cases were computed and validated using the results available in the literature. These included both propagation over flat terrain in a refractive and a non-refractive atmosphere, propagation over spherical earth, and propagation over a PEC knife edge placed on a perfectly conducting plane. Excellent agreement was observed and demonstrated for all cases. Also included, was a parametric study of the algorithm used, to show the effect of the horizontal step size Δx and the maximum height z_{\max} , for a fixed vertical step size Δz . The need for larger heights and smaller horizontal steps was demonstrated.

The model presented in this thesis can be applied to communication problems or

for target detection where prediction of propagation of HF/VHF signals over inhomogeneous and irregular terrain is highly desirable. Horizontal polarization applies mainly for radar systems. For this case, signals received from a target depend on the direct wave and the ground reflected wave. The latter ray's path depends on the terrain roughness and ground constants. It is also important to assess the atmospheric conditions. The numerical model developed in this thesis provides a useful tool for predicting the performance of a radar or communication system before its final development.

LIST OF REFERENCES

1. Thomson, D. J. and Chapman, N. R., "A Wide- Angle Split- Step Algorithm for the parabolic equation," *J. Acoustics Society Am.*, vol. 74(6), pp. 1848-1854, 1983.
2. Thompson, J. F., Warsi, Z. U. A., and Mastin, C. W., *Numerical Grid Generation*, North Holland, New York, 1985.
3. Dozier, B. L., "PERUSE: A Numerical Treatment of Rough Surface Scattering for the Parabolic Wave Equation," *J. Acoustics Society Am.*, vol. 75(5), pp. 1415-1432, 1982.
4. Kuttler, J. R. and Dockery, G. D., "Theoretical Description of the Parabolic Approximation/Fourier Transform Method of Representing Electromagnetic Propagation in the Troposphere," *Radio Science*, vol. 26, no.2, pp. 381-393, March-April 1991.
5. Janaswamy, R., Unpublished Notes, Naval Postgraduate School, Monterey, California.
6. Janaswamy, R., "A Rigorous Way of Incorporating Sea Surface Roughness Into the parabolic equation," Tech. Rep. NPS-EC-95-008, Naval Postgraduate School, Monterey, California, Sept. 1995.
7. Balanis, A. C., *Antenna Theory*, John Wiley & Sons, New York, pp.142 -144, 1982.
8. *Propagation of Radio Waves Through Standard Atmosphere*, Summary Technical Report of National Defence Research Committee, Vol. 3, 1946.
9. Anderson, L. J. and Trolese, L. G., "Simplified Method for Computing Knife Edge Diffraction in the Shadow Region," *IRE Trans. on Antennas and Propagation*, pp. 281-286, July 1958.

INITIAL DISTRIBUTION LIST

		No. of Copies
1.	Defence Technical Information Center 8725 John J. Kingman Rd., STE 0944 Ft. Belvoir, VA 22060-6218	2
2.	Dubley Knox Library Naval Postgraduate School 411 Dyer Rd. Monterey, CA 93943-5101	2
3.	Chairman, Code EC Department of Electrical and Computer Engineering Naval Postgraduate School Monterey, CA 93943-5101	1
4.	Professor Ramakrishna Janaswamy, Code EC/Js Department of Electrical and Computer Engineering Naval Postgraduate School Monterey, CA 93943-5101	5
5.	Professor Jeffrey B. Knorr, Code EC/Kn Department of Electrical and Computer Engineering Naval Postgraduate School Monterey, CA 93943-5101	1
6.	Mr. Kenneth Anderson NCCOSC RDTE DIV 543 53560 Hull Street San Diego, CA 92152-5001	1
7.	Ms. Amalia Barios NCCOSC RDTE DIV 543 53560 Hull Street San Diego, CA 92152-5001	1
8.	Mr. Herbert Hitney NCCOSC RDTE DIV 543 53560 Hull Street San Diego, CA 92152-5001	1

- | | | |
|-----|--|---|
| 9. | Mr. Richard Paulus
NCCOSC RDTE DIV 543
53560 Hull Street
San Diego, CA 92152-5001 | 1 |
| 10. | LT. Konstantinos Vlachos
104 Pindou Street
15669 Papagos
Athens, Greece | 5 |

DUDLEY KNOX LIBRARY
NAVAL POSTGRADUATE SCHOOL
MONTEREY CA 93943-5101

DUDLEY KNOX LIBRARY



3 2768 00323125 9